Radiative Kaon Capture at Rest in Hydrogen

D. A. Whitehouse,[2],[a] E. C. Booth,[2] W. J. Fickinger,[5] K. P. Gall[2],[b] M. D. Hasinoff,[3] N. P. Hessey,[1],[c] D. Horváth,[6] J. Lowe,[1] E. K. McIntyre,[2],[d] D. F. Measday,[3] J. P. Miller,[2] A. J. Noble,[3], B. L. Roberts,[2] D. K. Robinson,[5] M. Sakitt,[4] and M. Salomon[7]

[1]*University of Birmingham, Birmingham B15 2TT, United Kingdom*
[2]*Boston University, Boston, Massachusetts 02215*
[3]*University of British Columbia, Vancouver, British Columbia, Canada V6T 2A6*
[4]*Brookhaven National Laboratory, Upton, New York 11973*
[5]*Case Western Reserve University, Cleveland, Ohio 44106*
[6]*Central Research Institute for Physics of the Hungarian Academy of Sciences (KFKI), Budapest, Hungary and TRIUMF, Vancouver, British Columbia, Canada V6T 2A3*
[7]*TRIUMF, Vancouver, British Columbia, Canada V6T 2A3*

(Received 7 April 1989)

The photon spectrum from K^- stopping in liquid hydrogen has been measured with a high-resolution (1.5% FWHM at 300 MeV) NaI(Tl) detector. The branching ratios for $K^-p \to \Lambda\gamma$ ($E_\gamma = 281.4$ MeV) and $K^-p \to \Sigma^0\gamma$ ($E_\gamma = 219.5$ MeV) were obtained. The results are $R_{\Lambda\gamma} = (0.86 \pm 0.07^{+0.10}_{-0.08}) \times 10^{-3}$ and $R_{\Sigma^0\gamma} = (1.44 \pm 0.20^{+0.12}_{-0.10}) \times 10^{-3}$, where the first error is statistical and the second systematic. These results are not in good agreement with published predictions or with previous $\Lambda\gamma$ measurements.

PACS numbers: 14.20.Jn, 13.40.Hq, 13.75.Jz

The low-energy K^-p system has been the object of study for some years. Early in these investigations[1] it became evident that there might be a Y^* resonance below the 1432-MeV K^-p threshold. This $J^P = \frac{1}{2}^-$ state is now known as the $\Lambda(1405)$.

At first this resonance was identified as a K^-p bound state. With the advent of nonrelativistic constituent-quark models, such as the Isgur-Karl model,[2] it was postulated to be a three-quark configuration. However, its mass was not well predicted. The MIT bag model[3] predicts two low-lying $J^P = \frac{1}{2}^-$ states which might be identified with the $\Lambda(1405)$; however, a recent calculation by Umino and Myhrer[4] in a chiral bag model with broken $SU(2) \times SU(2)$ symmetry shows that one of these states moves up substantially in energy compared with the prediction of Ref. 3. The low-energy K^-p system has also been studied theoretically with a chiral $SU(3)_R \times SU(3)_L$ extension of the cloudy bag model.[5] In that model, calculations of the s-wave $\bar{K}N$ scattering cross sections indicate that the $\Lambda(1405)$ is dominantly a $\bar{K}N$ bound state. The recent K^-p data of Hemingway[6] show that the resonance shape is not well described by a Breit-Wigner line shape, but it is in agreement with the shape predicted by the cloudy bag model or K-matrix theory. After more than 25 years of investigation, the structure of the $\Lambda(1405)$ is still rather uncertain.

In both atomic and nuclear physics, studies of radiative decays of excited states have provided the key to our understanding of their structure. While radiative widths of a number of excited baryon states with $S = 0$ have been measured,[7] only the radiative decay of the $\Lambda(1520)$ excited state has been observed for $S = -1$ baryons. The published experiment of Mast *et al.*[8] suffered from low statistics as well as a substantial background, and the unpublished experiment of Bertini *et al.*[9] had rather poor photon-energy resolution and a large background. Consistent results were not obtained by the two groups.

The experiment reported below was performed to provide information on the radiative widths of the $\Lambda(1405)$ for the decays $\Lambda(1405) \to \Lambda\gamma$ and $\Lambda(1405) \to \Sigma^0\gamma$. The branching ratios $R_{\Lambda\gamma}$ and $R_{\Sigma^0\gamma}$ for the stopped-K^- reactions $K^-p \to \Lambda\gamma$ and $K^-p \to \Sigma^0\gamma$ were measured. To the extent that the participation of the intermediate $\Lambda(1405)$ in the radiative capture is understood, the radiative widths can be determined from the branching ratios.

Two theoretical calculations[10,11] of these branching ratios were carried out in anticipation of the results from this experiment. The Isgur-Karl model and the extended cloudy bag model were used, respectively. In both calculations, the radiative widths of the $\Lambda(1405)$ were taken from the respective models; however, it is difficult to compare the two calculations directly since they differ greatly in the choice of diagrams included.

In a complementary approach, two groups of authors[12,13] have used baryon-pole models to parametrize the radiative-capture branching ratios as a function of $\Lambda(1405)$ transition moments κ as defined below. The radiative width is given by[12,13]

$$\Gamma(\Lambda(1405) \to \Lambda\gamma) = \kappa^2 e^2 E_\gamma^3 / 4\pi M_p^2 .$$

An equivalent expression holds for the $\Lambda(1405) \to \Sigma^0\gamma$ width. All of the couplings were taken from experiment or symmetry relations except for the $\Lambda(1405)\Lambda\gamma$ and $\Lambda(1405)\Sigma^0\gamma$ vertices. The branching ratios are then calculated as a function of the transition moment, and this parametrization is compared with the experimental branching ratio to obtain κ.

At present there is disagreement between the various authors as to which diagrams should be used, and as to whether on-shell couplings will overestimate the contribution of the Born graphs. Also at issue is how the

denominator for the branching ratio, $K^- p \rightarrow$ anything, should be evaluated.[10,12,13]

The experiment was performed in the C8 low-energy separated beam at the Brookhaven National Laboratory Alternating Gradient Synchrotron (AGS). Kaons of momentum 680 MeV/c ($\Delta p/p = \pm 2\%$) were identified by six scintillation counters $S_{1\text{-}4}$ and $E_{1,2}$, a two-dimensional hodoscope H, plus a Čerenkov counter F which selected kaons (see Fig. 1). The K^- were slowed in a Cu degrader and were stopped in a liquid-hydrogen (LH_2) target 30.5 cm long and 20.3 cm in diameter. Pulse-height (dE/dx) information was obtained from E_1, E_2, and S_4 which was located immediately upstream of the target vacuum window. Events with multiple hits in the hodoscope or with the K^- in the outer portion of the beam envelope were rejected; the latter requirement minimized the background due to interactions in the target walls. A K-stop candidate was defined as the time coincidence of the beam counters, $S_1 \cdot S_2 \cdot F \cdot S_3 \cdot E_1 \cdot E_2 \cdot S_4$. On average, there were 250000 K^- incident on the degrader, 40000 survived the degrader, and 160900 stopped in the target per AGS beam burst.

Photons in time coincidence with a K-stop candidate were detected by a high-resolution NaI(Tl) detector[14] 55.9 cm deep and 49.5 cm in diameter. It was surrounded by a 12.7-cm-thick plastic-scintillator annular veto shield. To reject charged particles, the front was covered with a 2.5-cm-thick plastic scintillation counter. The data were taken during two different running periods. The detector viewed the target through a 12.7-cm-diam tungsten collimator, which was at 62.2 cm and 86.4 cm from the target center during the respective running periods.

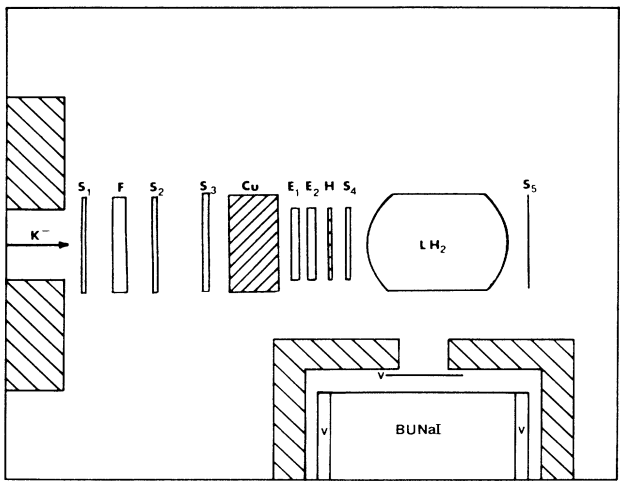

FIG. 1. A plan drawing of the experiment. The S_i were plastic scintillators, E_i were 1.26-cm-thick plastic scintillators used for dE/dx information, F was a velocity-selecting Čerenkov counter, and H was a 6×6-element hodoscope. The NaI detector was surrounded by 10 cm of steel and 7.6 cm of Pb.

The analog signals from each NaI phototube were clipped, and then charge integrated and digitized by LeCroy 2249W analog-to-digital converters (ADC's) with a gate width of 500 ns. Since such a long gate was necessary to obtained the best energy resolution, pulse pileup was carefully monitored. The pileup spectrum shape was measured on a continuous basis by triggering events randomly at ~10 Hz during the beam-on portion of the AGS cycle. The resulting spectrum was that of the ADC pedestal plus the pileup. This pileup shape was then used in the data analysis.

The detector energy calibration was determined by stopping π^- in the LH_2 target, and the intrinsic resolution was measured to be 1.3% FWHM for the 129.5-MeV Panofsky γ ray. The gain stability of the detector-electronics system was monitored with the monoenergetic π^+ from the reaction $K^- p \rightarrow \Sigma^- \pi^+$ ($T_\pi = 82.6$ MeV). The temperatures of the crystal and the analog electronics were also monitored. Data from periods where the temperature was not stable were discarded, as the energy resolution was significantly degraded. The remaining gain drifts were corrected with the information from the π^+ and the radiative-capture data from stopped π^-. A gain-corrected summed spectrum was produced for each detector geometry.

The neutron-induced and target-wall backgrounds were studied experimentally. Time-correlated low-energy neutrons were clearly separated from photons in a two-dimensional plot of energy versus the NaI(Tl) time relative to the K-stop candidate. The neutron background was negligible in the signal region of the spectrum. To obtain the shape of the spectrum from interactions in the target walls and vacuum vessel, the LH_2 was removed from the target and data were accumulated with all other conditions the same.

In the analysis of the data it was necessary to model the photon spectrum resulting from all the reaction channels of the $K^- p$ system plus other background processes (see Table I). Additional background contributions come from in-flight $K^- p \rightarrow Y\pi$ reactions, and the charge-exchange reaction $K^- p \rightarrow \bar{K}^0 n$ followed by $K_S \rightarrow \pi^0\pi^0$. The photon spectrum from each back-

TABLE I. The dominant reaction channels available to the $K^- p$ system at rest and secondary processes which produce photons. (The decay $\pi^0 \rightarrow \gamma\gamma$ is implied.) R denotes branching ratio.

Reaction	R	Ref.	Secondary reaction	R	Ref.
$\Lambda\pi^0$	0.07	15	$\Lambda \rightarrow n\pi^0$	0.358	16
$\Sigma^0\pi^0$	0.27	15	$\Sigma^0 \rightarrow \Lambda\gamma$	1.00	16
$\Sigma^+\pi^-$	0.19	15	$\Sigma^+ \rightarrow p\pi^0$	0.516	16
$\Sigma^-\pi^+$	0.47	15	$\Sigma^- p \rightarrow \Sigma^0 n$	0.42	17
			$\Sigma^- p \rightarrow \Lambda n$	0.58	17

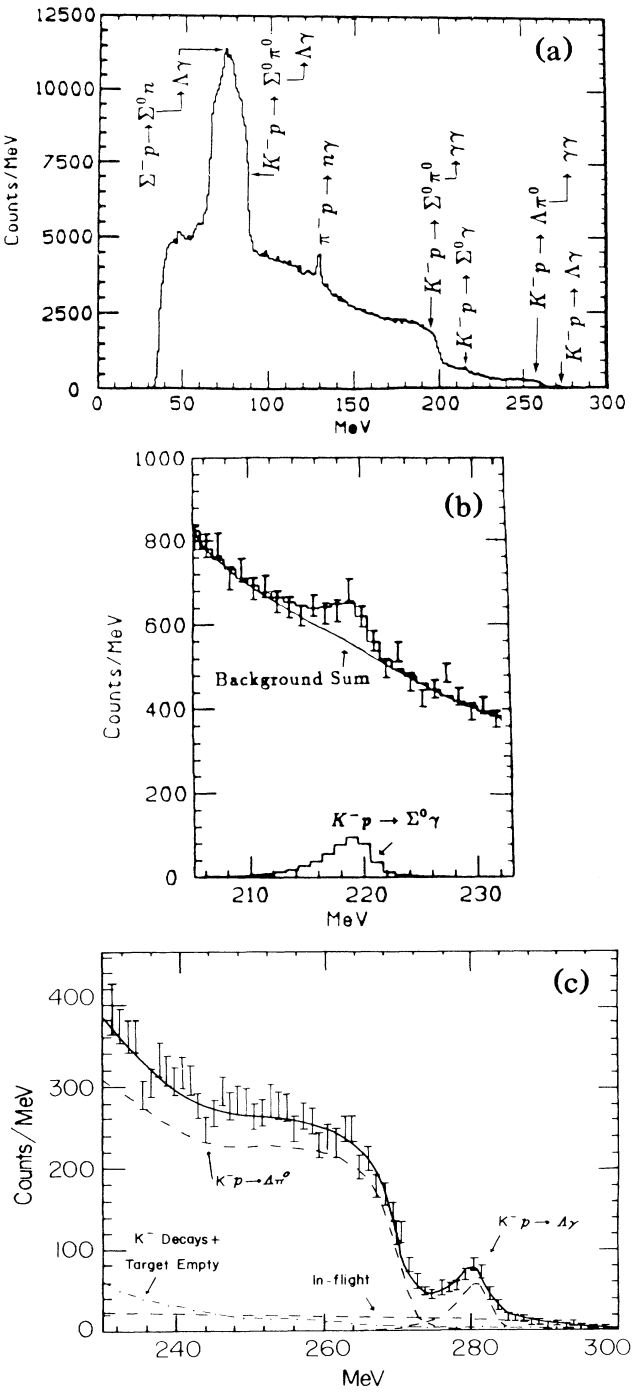

FIG. 2. (a) The experimental spectrum of data from one of the two running periods showing the two signal peaks plus backgrounds discussed in the text. (b) The region of the spectrum containing the $\Sigma^0\gamma$ signal. The smooth solid curve is the total background; the solid histogram is the fit to the data. The signal contribution to the fit is shown separately at the bottom of the figure. (c) The end-point region of the photon spectrum showing the $\Lambda\gamma$ radiative-capture peak and the end-point region of the π^0 decay photons from the $\Lambda\pi^0$ channel. The solid curve is the best fit. The background from K^- decays plus target empty is shown as a dot-dashed curve, while the contribution from in-flight interactions is shown by a dashed line. The latter are the dominant contribution above the end point. The $\Lambda\gamma$ signal contribution is shown as a separate dashed line.

ground channel was modeled with the relative intensities of the four stopped $K^- p \to Y\pi$ channels,[15] Σ^- charge exchange,[17] and the branching ratios for secondary decays[16] fixed at the published values. The Σ^0 from Σ^- charge exchange are lower in energy than those produced directly, $T_{\Sigma^0} = 1.6$ compared with 13.7 MeV, and thus the decay photons appear as a sharp peak on top of the broader distribution from the decay of directly produced Σ^0 [see Fig. 2(a)].

The NaI response function was modeled[14] with an EGS-based code which included estimates of the effects of crystal nonuniformities. This procedure produced line shapes in good agreement with measured spectra for electrons at 300 MeV and in excellent agreement for photons at 129 MeV.[14] The NaI line shapes and the measured pileup shapes were folded into the two calculated spectra which were then fitted to the gain-corrected spectra. Smearing from imperfect gain correction of the data was modeled by folding a Gaussian function into the calculated spectrum. The width of this Gaussian obtained from fits to the data was found to be small, 0.8% for one data set and 0% for the other.

In addition to the overall normalization of the $Y\pi$ channels and the signal-channel amplitudes, the free parameters in the fit included the amplitudes for $K^- \to \pi^-\pi^0$, Σ^- charge exchange, and in-flight $Y\pi$ reactions, the amplitude for $\pi^- p \to n\gamma$ or $n\pi^0$, as well as contributions from the target-empty and neutron backgrounds. The total number of stopped $K^- p$ interactions was determined from a fit to the $\Lambda\pi^0$ "shoulder" [see Fig. 2(a)] over the energy range 230–285 MeV. Consistent results were obtained for fits to the $\Sigma^0\pi^0$ "shoulder" and the $\Sigma^0 \to \Lambda\gamma$ peak which dominates the low-energy region of the spectrum [Fig. 2(a)]. The results quoted below were obtained using the $\Lambda\pi^0$ channel for normalization.

The systematic errors studied in the analysis included uncertainties in the following: the Gaussian width introduced by gain correction, the small disagreement between the predicted and measured low-energy tail observed in the NaI response to 330-MeV electrons,[14] the branching ratio for the $\Lambda\pi^0$ channel, and the shape of the momentum spectrum of K^- which react in flight. For example, it is this latter uncertainty which dominates, and gives systematic errors of $^{+0.08}_{-0.04} \times 10^{-3}$ and $^{+0.06}_{-0.02} \times 10^{-3}$ for the two $\Lambda\gamma$ data sets.

In Fig. 2(a) the entire photon spectrum is shown. In addition to the two signal channels and the Σ^0 decay photons, the sharp edges of the distributions of π^0 decay photons from $K^- p \to \Sigma^0\pi^0$ at 205 MeV and $K^- p \to \Lambda\pi^0$ at 271 MeV can be seen. In Figs. 2(b) and 2(c)

TABLE II. Experimental and theoretical radiative-capture branching ratios. For this experiment, the first error is statistical and the second is systematic. All branching ratios (R) are in units of 10^{-3}.

	Experiment			Theory	
R	Present	Ref. 18	Ref. 19	Ref. 10	Ref. 11
$R_{\Lambda\gamma}$	$0.86 \pm 0.07^{+0.10}_{-0.08}$	2.8 ± 1.4	2.8 ± 0.8	3.4	1.9
$R_{\Sigma^0\gamma}$	$1.44 \pm 0.20^{+0.12}_{-0.10}$	...	...	2.6	2.3
$\frac{R_{\Sigma^0\gamma}}{R_{\Lambda\gamma}}$	1.71 ± 0.30	...	...	0.76	1.2

the two signal regions are shown. The solid curve represents a best fit of the calculated spectrum to the data. The detector response to monoenergetic photons, which was calculated with EGS,[14] can be seen in Figs. 2(b) and 2(c) where the signal channels (plus pileup) are plotted separately at the bottoms of the figures.

The branching ratios obtained are given in Table II along with $\Lambda\gamma$ results from two earlier experiments[18,19] and the theoretical predictions. A total of 499 $\Lambda\gamma$ events and 850 $\Sigma^0\gamma$ events were observed. Neither of the previous experiments[18,19] obtained as clear an identification of the $\Lambda\gamma$ channel as is obtained in the present experiment. Our data suggest that with the poor energy resolution available previously, most of the events formerly attributed to radiative capture at rest were either from in-flight $\Lambda\pi^0$ production or pileup.

As for the recent calculations,[10,11] neither agrees with our measured branching ratios. However, if one takes the ratio of the two branching ratios, where some of the theoretical uncertainties cancel, the chiral bag model comes closer. Two additional calculations are in progress.[20,21] The pole-model calculation of Workman and Fearing[13] is compatible with our data for the value of the transition moment, $\kappa_\Lambda \simeq -0.35$ and $\kappa_\Sigma \simeq -0.2$ or $+0.65$. In the nonrelativistic quark model if the $\Lambda(1405)$ is a pure SU(3) singlet, then $\kappa_\Sigma = \sqrt{3}\kappa_\Lambda$ which is clearly not the case experimentally.

In principle, the pole-model calculations[12,13] should permit one to obtain a radiative width directly from the branching ratio. As mentioned above, this is not yet possible because of theoretical questions currently under study. A resolution of these issues is expected in the near future.

We wish to thank D. Lowenstein, D. Lazarus, and the AGS staff for their support of this experiment; R. Meier and the AGS target group for the design, construction, and operation of the LH_2 target; and R. C. Barrett, R. H. Dalitz, H. W. Fearing, N. Isgur, B. K. Jennings, A. W. Thomas, and Y. Umino for helpful discussions of the theory. We thank B. Bassalleck, J. F. Skelly, S. Stanislaus, W. VanRiper, C. E. Waltham, and D. W. Warner for their participation in portions of the experiment. This work was supported in part by the U.S. NSF and DOE, the United Kingdom Science and Engineering Research Council, and the Canadian Natural Sciences and Engineering Research Council.

[a]Present address: Los Alamos Meson Physics Facility, Los Alamos, NM 87545.

[b]Present address: Department of Radiation Medicine, Massachusetts General Hospital, Boston, MA 02114.

[c]Present address: Rutherford Appleton Laboratory, Chilton, Didcot, Oxon OX11 0QX, United Kingdom.

[d]Present address: Eaton Corporation, Beverly, MA 01915.

[1]R. H. Dalitz and S. F. Tuan, Ann. Phys. (N.Y.) **3**, 307 (1960); R. H. Dalitz, T. C. Wong, and G. Rajasekaran, Phys. Rev. **153**, 1617 (1967).

[2]N. Isgur and G. Karl, Phys. Lett. **72B**, 109 (1977); **74B**, 353 (1978); Phys. Rev. D **18**, 4187 (1978); **19**, 2653 (1979); **20**, 1191 (1979); L. A. Copley, N. Isgur, and G. Karl, Phys. Rev. D **20**, 768 (1979).

[3]See for example, A. W. Thomas, Adv. Nucl. Phys. **13**, 1 (1983), and references therein.

[4]Y. Umino and F. Myhrer, Phys. Rev. D **39**, 3391 (1989).

[5]E. A. Veit, B. K. Jennings, R. C. Barrett, and A. W. Thomas, Phys. Lett. B **137**, 415 (1984); Phys. Rev. D **31**, 1033 (1985); E. A. Veit, A. W. Thomas, and B. K. Jennings, Phys. Rev. D **31**, 2242 (1985).

[6]R. J. Hemingway, Nucl. Phys. **B253**, 742 (1985).

[7]F. Foster and G. Hughes, Rep. Prog. Phys. **46**, 1445 (1983).

[8]T. L. Mast *et al.*, Phys. Rev. Lett. **25**, 1715 (1968).

[9]R. Bertini *et al.*, contribution to the Tenth International Conference on Particles and Nuclei (PANIC 10), Heidelberg, 1984 (unpublished), contributed paper M18. These data have not been subsequently published.

[10]J. D. Darewych, R. Koniuk, and N. Isgur, Phys. Rev. D **32**, 1765 (1986). An important diagram was omitted in this calculation, and a new calculation is in progress.

[11]Y. S. Zhong, A. W. Thomas, B. K. Jennings, and R. C. Barrett, Phys. Rev. D **38**, 837 (1988).

[12]H. Burkhardt, J. Lowe, and A. S. Rosenthal, Nucl. Phys. **A440**, 653 (1985).

[13]R. L. Workman and H. W. Fearing, Phys. Rev. D **37**, 3117 (1988).

[14]J. P. Miller *et al.*, Nucl. Instrum. Methods Phys. Res., Sect. A **270**, 431 (1988).

[15]D. J. Miller, R. J. Nowak, and T. Tymieniecka, in *Low and Intermediate Energy Kaon-Nucleon Physics,* edited by E. Ferrari and G. Violini (Reidel, Dordrecht, 1980).

[16]Particle Data Group, M. Aguilar-Benitez *et al.*, Phys. Lett. **170B**, 1 (1986).

[17]M. Goossens *et al.*, in Ref. 15.

[18]W. E. Humphrey and R. R. Ross, Phys. Rev. **127**, 1305 (1962).

[19]J. Lowe *et al.*, Nucl. Phys. **B209**, 16 (1982).

[20]N. Isgur (private communication).

[21]Y. Umino (private communication).